PAN
ARCHIVES OF ACOUSTICS
Vol. **46**, No. 2, pp. 335–340 (2021)
DOI: 10.24425/aoa.2021.136587

Research Paper

Broadening Low-Frequency Band Gap of Double-Panel Structure Using Locally Resonant Sonic Crystal Comprised of Slot-Type Helmholtz Resonators

Myong-Jin KIM*, Chun-Gil RIM, Kyong-Su WON

Institute of Acoustics
Department of Physics
Kim Il Sung University
Pyongyang, Democratic People's Republic of Korea
*Corresponding Author e-mail: mj.kim0903@ryongnamsan.edu.kp

(*received June 24, 2020; accepted December 16, 2020*)

An approach is presented to form and broaden the low-frequency band gap of the double panel structure (DPS) by using a locally resonant sonic crystal (LRSC) in this work. The LRSC is made of cylindrical Helmholtz resonators arranged on square lattice. Their designs are similar to a slot-type resonator, but have different depths of slot. Elongating the slit neck inward and distributing the depths of slots produce a broad local resonant band gap at low frequencies: an average insertion loss (IL) of 10.9 dB covering 520 Hz to 1160 Hz with a LRSC of 12 cm width. Next, the effect of porous material filled into the resonators on the local resonant band gap is evaluated. It is shown that filling of porous material into the resonators decreases the height and width of the local resonant band gap. Finally, the transmission losses (TLs) through the DPS with LRSC are calculated as a function of the incident angle of the sound wave for LRSC embedded in porous material and not. The results show that the porous material can be significantly reduce the incident angle dependency of TL through the DPS with LRSC.

Keywords: sound transmission loss; locally resonant sonic crystal; double-panel structure; sound insulation.

1. Introduction

According to the mass law, heavy and thick materials must be used to achieve a high sound insulation. However, this is limited due to the demand of lightweight design. One way to overcome this shortcoming is to employ the multilayer panel structure. The double-panel structures (DPSs) are usually used in buildings and vehicles and they provide good sound insulation in a wide frequency band. Xin *et al.* (2008) studied the vibro-acoustic performance of double-panel partition with enclosure air cavity analytically and experimentally. The double-panel with multilayer absorbent blankets was studied analytically (Doutres, Atalla, 2010) and the effect of vertical metal studs placed between two panels on sound transmission loss (STL) was modelled theoretically (Wang *et al.*, 2005). Arjunan *et al.* (2014) evaluated the sound attenuation of a stud-based double-panel by 3D vibro-acoustic FE modeling. Kang and Bolton (1996) conducted a theoretical study of a double panel lined with foams. Bolton *et al.* (1996) performed a theoretical modeling of sound transmission through the infinite DPS with porous material in the diffuse sound field. Panneton and Atalla (1996) and Sgard *et al.* (2000) calculated STLs through a finite double panel lined with porous materials for the arbitrary incidence using FE (Finite Element) method and BE (Boundary Element) method. Tanneau *et al.* (2006) used genetic algorithms to optimize multilayered panel structures consisting of solid, fluid and porous materials.

Sonic crystal (SC) is made of periodically arranged solid scatterers placed in fluid including water and air. Sound wave with a wavelength equal to half the lattice constant cannot propagate through SC due to the destructive interference. Martínez-Sala *et al.* (1995) performed the first experimental work on the sound attenuation by periodic structure. Later on, Sanchez-Perez *et al.* (2002) showed that periodical scatter arrays provide noticeable sound attenuations. Morandi

et al. (2016) performed a free-field measurement over the sound insulation and reflection of SC noise barriers according to the European standards EN 1793-2, EN 1793-5 and EN 1793-6. Garcia-Raffi *et al.* (2018) showed a significant noise attenuation using a SC comprised of solid scatterers in water. Guild *et al.* (2018) fabricated a sound absorber constructed of a woven arrangement of SCs and showed the presence of zero transmittance over a given frequency range.

Many researches have been done to broaden the band gap by using LRSC. Sanchez-Dehesa *et al.* (2011) proposed a noise barrier consisted of three rows of perforated metal shells filled with rubber crumb. Chalmers *et al.* (2009) showed the potential for sound shielding in the audible frequency range using a simply mixed array and a concentric array of scatterers. Cavalieri *et al.* (2019) have numerically and experimentally investigated the broadband attenuation performance of a 3D LRSC due to the couple of multiple resonances and the Bragg band gap.

Recently, researches has been conducted to enhance the sound insulation performance of multilayer structure by applying the sonic crystal. In a DPS, SCs produce a wide Bragg-type band gap due to the it periodicity as in free field and inhibit the generation of "standing-wave" resonances in regions of two panels, resulting in the improvement of overall sound insulation compared to the counterparts with the same total size. Gulia and Gupta (2018) studied the combined effect of SC and glass wool inserted between two panels and showed that DSP with SC embedded in glass wool gives the best sound insulation. Kim (2019a) extended the previous work (Gulia, Gupta, 2018) to address the problem of a triple-panel structure and showed that the triple-panel structure has a potential to provide better soundproofing properties than DPS counterpart, reducing the overall weight. Qian (2018) proposed the locally resonant phononic crystal (LRPC) composite DPS with periodically attached pillars and etched holes and investigated the band gap properties of the structure by using FEM. Kim (2019b) proposed a LRSC consisted of "C"-shaped Helmholtz resonator columns with different resonant frequencies to enhance the sound insulation of DPS in the low frequency range. Gulia and Gupta (2019) reported that combining the properties of LRSC and porous material produce better low-frequency sound insulation of the triple panel as well as in high frequency range.

The low-frequency noise is widely existed in human living environment, but somewhat difficult to control by using traditional methods because of the long wavelength and strong penetrability of low-frequency waves. In this work, one type of LRSC is presented to form and broaden a low-frequency band gap of a DPS. The LRSC consists of three columns of Helmholtz resonators, each of which has a different resonant frequency corresponding the slot depth. Calculations are conducted in the FE software ANSYS Multiphysics (v18.0) acoustic package. Three local resonance band gaps are overlapped in the low frequencies, resulting in formation of a broadband of sound insulation. In addition, porous material are filled between two panels and inside of the resonators to study the effect of the porous materials on the low-frequency band gap and the dependence of DPS sound insulation on the incident angle.

2. FE modeling

A numerical model of DPS with a periodic array of slot-type Helmholtz resonator (SHR) was developed as follows. Three SHRs in the z-direction were considered, as shown in Fig. 1, where d_1, d_2, d_3 are the slot depths of each rows. A periodic boundary condition was applied in the x-direction of the domain to reduce the computational cost required to solve the FE model, thus extending the length of the structure to infinity in the positive and negative x-directions.

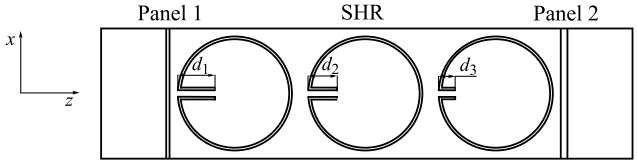

Fig. 1. FE model of DPS with 3 rows of SHR.

Aluminum sheets were used for two parallel panels. Material properties of aluminum are density of 2700 kg/m^3, Young's modulus of 70 GPa and Poison's ratio of 0.33. The distance between two panels is 12 cm and their thicknesses are 1 mm and 2 mm, respectively. The density and the sound speed of air are $\rho_0 = 1.25$ kg/m^3 and $c_0 = 343$ m/s, respectively.

SHR were assumed to be made of aluminum with thickness of 0.2 mm. Outer radius of resonator is 17.5 mm and lattice constant (distance between centers of neighbor scatterers) is 40 mm. The surfaces of scatterers were considered to be free to take account of the vibration of very thin shell.

Porous materials provide high sound absorption, especially at high frequencies. The acoustic performance of porous materials were modelled in various ways including empirical, analytical, semi-phenomenological, etc. models. Glass wool was taken as a porous material and the Delany-Bazley model (Delany, Bazley, 1970) was employed to model the glass wool. According to the Delany-Bazley model, wave number k_g and characteristic impedance z_g of the glass wool are described, respectively, as follows:

$$k_g = \frac{\omega}{c_0}\left[1 + 0.0978\chi^{-0.7} - j0.189\chi^{-0.595}\right], \quad (1)$$

$$z_g = \rho_0 c_0\left[1 + 0.0571\chi^{-0.754} - j0.087\chi^{-0.732}\right], \quad (2)$$

where $\chi = \frac{\rho_0 f}{R_g}$, ρ_0 and c_0 are the density and sound speed of fluid in the absence of the porous material, f is the frequency, ω is the angular frequency, and R_g is the flow resistivity of glass wool. Mean fiber diameter d_g and density ρ_g of glass wool are 10 μm and 12 kg/m^3 respectively. Flow resistivity can then be calculated as (Bies, Hansen, 1980)

$$R_g = \frac{3.18 \cdot 10^{-9} \rho_g^{1.53}}{d_g^2}. \tag{3}$$

The plane wave incidence condition was applied to left boundary. Left and right sides of DPS were assumed to be infinite radiation boundaries. There is no backward reflection at those two boundaries and then following boundary conditions are satisfied (Gulia, Gupta, 2018).

$$\left(-\frac{\nabla p}{\rho}\right) \cdot \mathbf{n} = \frac{i\omega}{\rho c_c} p - \frac{i\omega}{\rho c_c} p_0, \tag{4}$$

$$\left(-\frac{\nabla p}{\rho}\right) \cdot \mathbf{n} = \frac{i\omega}{\rho c_c} p, \tag{5}$$

where p is the sound pressure, $p = p_0 e^{ikr}$, k is the wave vector, r is the direction vector, ρ is the density, $\mathbf{n}$ is the normal vector, and c_c is the sound speed.

Harmonic analysis was performed in the range of 20–6000 Hz with the frequency interval of 20 Hz. The model was meshed with an element size (about 5 mm) of one-tenth of the minimum wavelength. STL is considered to be average sound power difference on the left side and the right side of the DPS.

3. Results and discussion

The resonant frequency of a split ring resonator (SRR) is given by Chalmers *et al.* (2009):

$$f = \frac{c}{2\pi} \sqrt{\frac{\sigma}{S\left(L + \frac{1}{2}\sqrt{\pi\sigma}\right)}}, \tag{6}$$

where L is the neck length , σ is the slot width, and S is the inner cross-sectional area.

Change the volume of the air cavity or width of the slot, and the resonance frequency changes. Figure 2a shows the Helmholtz resonance frequency of the SRR with outer diameter of 35 mm and thickness of 0.2 mm with varying the slot width in the range of 0.4–14 mm. And Fig. 2b shows the sound transmission loss through the DPS for slot width of 0.4 mm. It can be observed in Fig. 2 that all the resonance frequencies are higher than 1000 Hz. TL shows a broad band gap around the Bragg frequency, due to the periodicity of the resonators, and a relatively sharp band gap around the local resonant frequency.

From Eq. (6), it is necessary to increase the neck length to reduce the resonance frequency. However, slot

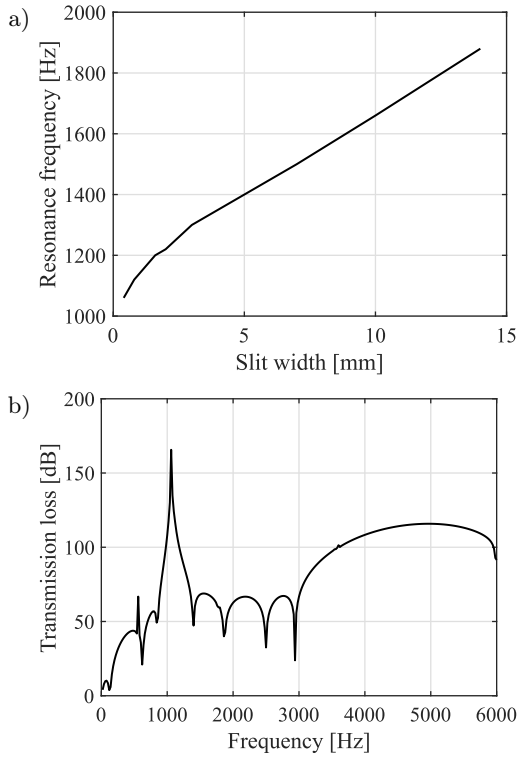

Fig. 2. Helmholtz resonance frequency as a function of slot width of SRR (a) and TL curve for slot width of 0.4 mm (b).

can't be elongated outward of the resonator because of the demand of filling fraction of SC. This limitation can be overcome by elongating the slot inward as shown in Fig. 1.

For the slot width of 0.4 mm, the resonance frequencies with varying the slot depth from 1 mm to 6 mm are as in Fig. 3. It is possible to decrease the resonance frequency to about 500 Hz by setting the slot depth to be 6 mm.

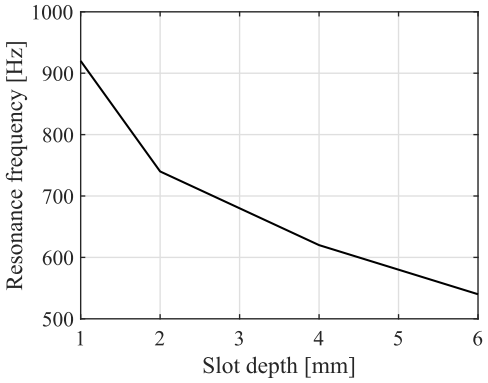

Fig. 3. Helmholtz resonance frequency as a function of slot depth of SHR.

Figure 4 shows STL through the DPS with the LRSC, where all the slot depths are 6 mm, *versus* that through the DPS with air cavity between the two panels. Two types of band gaps, i.e., Bragg-type band gap

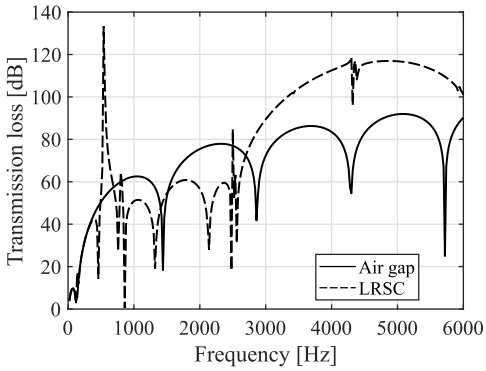

Fig. 4. TL through DPS with LRSC and that with air cavity.

and the resonant band gap can be obviously seen from the figure.

To explorer the coupled effect of LRSC and porous material on the low-frequency sound insulation, glass wool was inserted into the air domain between two panels. Figure 5 shows TLs of DPSs inserted with glass wool between two panels. Solid line represents the TL for DPS without LRSC, dash dotted line for one with glass wool inserted into all the air domain (LRSC-2) and dashed line for one with glass wool inserted between the panels and scatterers (LRSC-1). For all the cases, the slot depth is 6 mm.

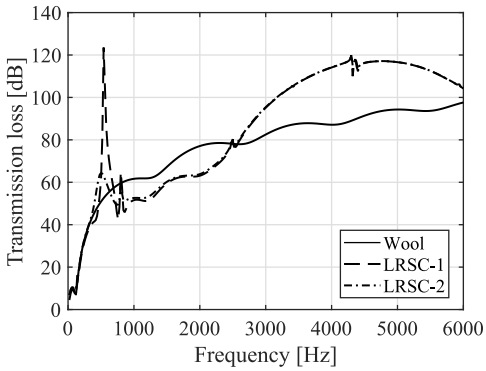

Fig. 5. TLs through DPSs with glass wool filling between two panels.

DPS with LRSC provides superior sound insulation around Bragg frequency (2500–6000 Hz in this work). However, if the glass wool is inserted into the inside of resonators, the resonant band gap reduce noticeably (dash dotted line), so that local resonance have little effect on the sound insulation and TL around the Helmholtz resonance frequency compares with that without LRSC.

Decreasing the number of resonator rows to 2 and increasing the lattice constant by 1.5 times, Bragg-type band gap moves downward, which might results in the enhancement of the sound insulation in the range between the resonant band gap and Bragg-type band gap. Figure 6 shows TL curve of DPS with two rows of

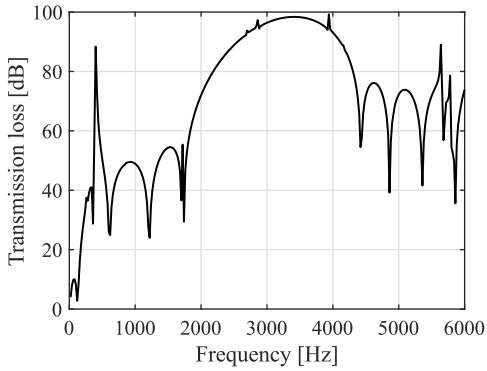

Fig. 6. TL through DPS with 2 rows of resonators.

resonators, where outer radius is 52.5 mm, thickness 0.25 mm, slot depth 6 mm, slot width 0.4 mm and lattice constant 60 mm.

However, it results in lowering the peak of the Bragg-type band gap (by about 20 dB in Figs 4 and 6). Then, considering the fact that the width of resonant band gap is narrow, decreasing the number of resonator rows gives small possibility to broaden the low-frequency band gap. Thus, the most way is to distribute rationally the resonance frequencies of each 3 rows so as to overlap with each other.

Figure 7 shows the TLs of three configurations, i.e., DPS with air cavity (dash dotted line), DPS with LRSC (solid line) and DPS with LRSC embedded in

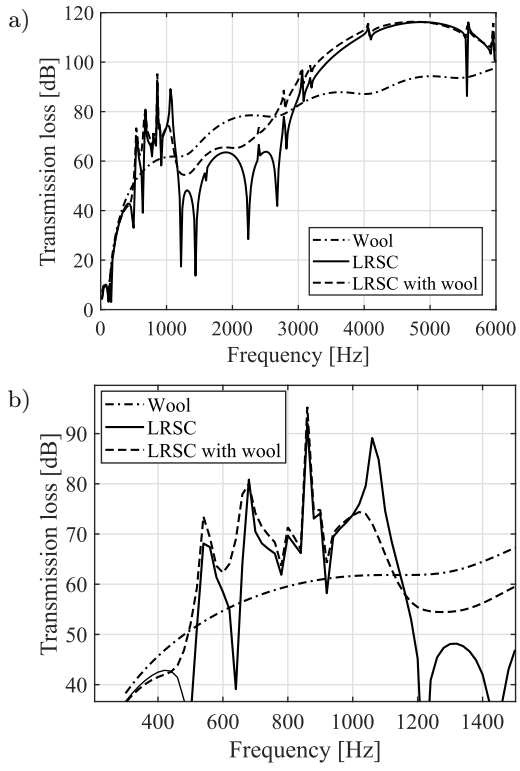

Fig. 7. TLs of three configurations of DPS in the range of 20–6000 Hz (a) and around the local resonant frequencies (b).

glass wool (dashed line). The slot depths of three rows are 6 mm, 3 mm, and 0.2 mm (thickness of shells), respectively. Figure 7b represents TL curves around the local resonance frequencies.

It can be seen that DPS with LRSC provides sound insulation, on average, 10.9 dB higher than that with glass wool filling in the range of 520–1160 Hz. However, the soundproofing performance of the DPS with LRSC decreases by 8 dB in the range of 1160–2260 Hz.

Sound wave does not always enter the structure not only in a specified direction such as normal direction, but also diffusely. Thus, it is important to eliminating the dependence of sound insulation on the incidence angle of sound wave.

Figure 8 shows TLs through DPS with LRSC-glass wool assembly and with LRSC at frequencies of 1000 Hz (Fig. 8a) and 1440 Hz (Fig. 8b), which are corresponding to the lowest peak and dip (the first "standing-wave" resonance) in the solid line of Fig. 4.

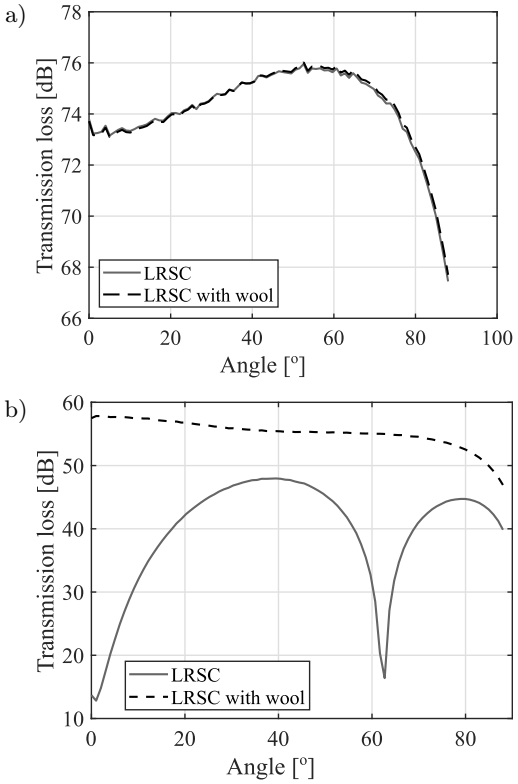

Fig. 8. Incidence angle dependency of sound insulation at frequencies of 1000 Hz (a) and 1440 Hz (b).

Figure 8a shows that glass wool gives little effect on the incidence angle dependency of sound insulation of DPS with LRSC at frequency corresponding to the peak of TL curve. However, it influences significantly the dependence of sound insulation on the incidence angle at frequencies corresponding to the dips of TL curve as in Fig. 8b. For DPS with LRSC embedded in glass wool, the deviation of TL is less than 10 dB in the entire range of incidence angle, but it is several tens dB for DPS without glass wool. This is also true for DPS without SC.

4. Conclusions

A LRSC based on the slot-type resonators has been proposed to enhance the low-frequency sound insulation of DPS, where slots are elongated into the cylindrical shell and have different slot depths for each rows. Through FE simulations on the several configurations, it is verified that it is possible to form a broad resonant band gap in a low frequency range by regulating and distributing the slot depths of LRSC inserted into the DPS. In addition, the simulation results show that glass wool should not be filled into the Helmholtz resonators, but only between the panels and scatterers. Glass wool filling into the resonators decreases markedly the height of the resonant band gap. Finally, it is found that LRSC in DPS should be embedded in porous material to reduce the dependence of the sound transmission on the incidence angle of sound wave. Filling the glass wool gives the deviation of TL less than 10 dB with varying the incidence angle from 0 to 90 degrees. The width of the local resonant band depends on the friction of the system. Larger frictions gives the wider band gap. Thus, the resonant band gap will be broadened further by increasing the roughness of slot surface in applications.

Acknowledgments

We would like to acknowledge the co-workers of Institute of Acoustics, Department of Physics, Kim Il Sung University for their helpful discussions and constructive remarks.

References

1. Arjunan A., Wang C.J., Yahiaoui K. (2014), Development of a 3D finite element acoustic model to predict the sound reduction index of stud based double-leaf walls, *Journal of Sound and Vibration*, **333**(23): 6140–6155, doi: 10.1016/j.jsv.2014.06.032.

2. Bies D.A., Hansen C.H. (1980), Flow resistance information for acoustical design, *Applied Acoustics*, **13**(5): 357–391, doi: 10.1016/0003-682X(80)90002-X.

3. Bolton J.S., Shiau N.M., Kang Y.J. (1996), Sound transmission through multi–panel structures lined with elastic porous materials, *Journal of Sound and Vibration*, **191**(3): 317–347, doi: 10.1006/jsvi.1996.0125.

4. Cavalieri T., Cebrecos A., Groby J.-P., Chaufour C., Romero-García V. (2019), Three-dimensional multiresonant lossy sonic crystal for broadband acoustic attenuation: Application to train noise reduction, *Applied Acoustics*, **146**: 1–8, doi: 10.1016/j.apacoust.2018.10.020.

5. Chalmers L., Elford D.P., Kusmartsev F.V., Swallowe G.M. (2009), Acoustic band gap formation in two-dimensional locally resonant sonic crystals comprised of Helmholtz resonators, *International Journal of Modern Physics B*, **23**: 4234–4243, doi: 10.1142/9789814289153_0023.

6. Delany M.E., Bazley E.N. (1970), Acoustical properties of fibrous absorbent materials, *Applied Acoustics*, **3**(2): 105–116, doi: 10.1016/0003-682X(70)90031-9.

7. Doutres O., Atalla N. (2010), Acoustic contributions of a sound absorbing blanket placed in a double panel structure: Absorption versus transmission, *The Journal of the Acoustical Society of America*, **128**(2): 664–671, doi: 10.1121/1.3458845.

8. Garcia-Raffi L.M. *et al.* (2018), Broadband reduction of the specular reflections by using sonic crystals: A proof of concept for noise mitigation in aerospace applications, *Aerospace Science and Technology*, **73**: 300–308, doi: 10.1016/j.ast.2017.11.048.

9. Guild M.D., Rothko M., Sieck C.F., Rohde C., Orris G. (2018), 3D printed sound absorbers using functionally–graded sonic crystals, *The Journal of the Acoustical Society of America*, **143**(3): 1714–1714, doi: 10.1121/1.5035582.

10. Gulia P., Gupta A. (2018), Enhancing the sound transmission loss through acoustic double panel using sonic crystal and porous material, *The Journal of the Acoustical Society of America*, **144**(3): 1435–1442, doi: 10.1121/1.5054296.

11. Gulia P., Gupta A. (2019), Sound attenuation in triple panel using locally resonant sonic crystal and porous material, *Applied Acoustics*: **156**, 113–119, doi: 10.1016/j.apacoust.2019.07.012.

12. Kang Y.J., Bolton J.S. (1996), A finite element model for sound transmission through foam lined double panel structure, *The Journal of the Acoustical Society of America*, **99**(5): 2755–2755, doi: 10.1121/1.414856.

13. Kim M.-J. (2019a), Improving sound transmission through triple-panel structure using porous material and sonic crystal, *Archives of Acoustics*, **44**(3): 533–541, doi: 10.24425/aoa.2019.129268.

14. Kim M.-J. (2019b), Numerical study for increasement of low frequency sound insulation of double-panel structure using sonic crystals with distributed Helmholtz resonators, *International Journal of Modern Physics B*, **33**(14): 1950138, doi: 10.1142/S0217979219501388.

15. Martínez-Sala R., Sancho J., Sánchez J.V., Gómez V., Llinares J., Meseguer F. (1995), Sound attenuation by sculpture, *Nature*, **378**(6554): 241–241, doi: 10.1038/378241a0.

16. Morandi F., Miniaci M., Marzani A., Barbaresi L., Garai M. (2016), Standardised acoustic characterisation of sonic crystals noise barriers: Sound insulation and reflection properties, *Applied Acoustics*, **114**: 294–306, doi: 10.1016/j.apacoust.2016.07.028.

17. Panneton R., Atalla N. (1996), Numerical prediction of sound transmission through finite multilayer systems with poroelastic materials, *The Journal of the Acoustical Society of America*, **100**(1): 346–354, doi: 10.1121/1.415956.

18. Qian D. (2018), Wave propagation in a LRPC composite double panel structure with periodically attached pillars and etched holes, *Archives of Acoustics*, **43**(4): 717–725, doi: 10.24425/aoa.2018.125165.

19. Sanchez-Dehesa J., Garcia-Chocano V.M., Torrent D., Cervera F., Cabrera S., Simon F. (2011), Noise control by sonic crystal barriers made of recycled materials, *The Journal of the Acoustical Society of America*, **129**(3): 1173–1173, doi: 10.1121/1.3531815.

20. Sanchez-Perez J.V., Rubio C., Martinez-Sala R., Sanchez-Grandia R., Gomez V. (2002), Acoustic barriers based on periodic arrays of scatterers, *Applied Physics Letters*, **81**(27): 5240–5242, doi: 10.1063/1.1533112.

21. Sgard F.C., Atalla N., Nicolas J. (2000), A numerical model for the low frequency diffuse field sound transmission loss of double-wall sound barriers with elastic porous linings, *The Journal of the Acoustical Society of America*, **108**(6): 2865–2872, doi: 10.1121/1.1322022.

22. Tanneau O., Casimir J.B., Lamary P. (2006), Optimization of multilayered panels with poroelastic components for an acoustical transmission objective, *The Journal of the Acoustical Society of America*, **120**(3): 1227–1238, doi: 10.1121/1.2228663.

23. Wang J., Lu T.J., Woodhouse J., Langley R.S., Evans J. (2005), Sound transmission through lightweight double-leaf partitions: Theoretical modelling, *Journal of Sound and Vibration*, **286**(4–5): 817–847, doi: 10.1016/j.jsv.2004.10.020.

24. Xin F.X., Lu T.J., Chen C.Q. (2008), Vibroacoustic behavior of clamp mounted double-panel partition with enclosure air cavity, *The Journal of the Acoustical Society of America*, **124**(6): 3604–3612, doi: 10.1121/1.3006956.